

Original Research

Linking Disulfide Levels and NAD⁺ Metabolism with Alzheimer's Disease for Diagnostic Modeling and Target Drug Analysis

Yanbing Wang¹, Lining Su^{2*}, Yongcai Zhang², Huiping Wei²¹Department of Sports, Hebei North University, 075000 Zhangjiakou, Hebei, China²Department of Basic Medicine, Hebei North University, 075000 Zhangjiakou, Hebei, China*Correspondence: 343376274@qq.com (Lining Su)

Academic Editor: Rafael Franco

Submitted: 17 June 2023 Revised: 15 September 2023 Accepted: 18 September 2023 Published: 22 April 2024

Abstract

Background: Alzheimer's disease (AD) is a condition that affects the nervous system and that requires considerably more in-depth study. Abnormal Nicotinamide Adenine Dinucleotide (NAD⁺) metabolism and disulfide levels have been demonstrated in AD. This study investigated novel hub genes for disulfide levels and NAD⁺ metabolism in relation to the diagnosis and therapy of AD. **Methods:** Data from the gene expression omnibus (GEO) database were analyzed. Hub genes related to disulfide levels, NAD⁺ metabolism, and AD were identified from overlapping genes for differentially expressed genes (DEGs), genes in the NAD⁺ metabolism or disulfide gene sets, and module genes obtained by weighted gene co-expression network analysis (WGCNA). Pathway analysis of these hub genes was performed by Gene Set Enrichment Analysis (GSEA). A diagnostic model for AD was constructed based on the expression level of hub genes in brain samples. CIBERSORT was used to evaluate immune cell infiltration and immune factors correlating with hub gene expression. The DrugBank database was also used to identify drugs that target the hub genes. **Results:** We identified 3 hub genes related to disulfide levels in AD and 9 related to NAD⁺ metabolism in AD. Pathway analysis indicated these 12 genes were correlated with AD. Stepwise regression analysis revealed the area under the curve (AUC) for the predictive model based on the expression of these 12 hub genes in brain tissue was 0.935, indicating good diagnostic performance. Additionally, analysis of immune cell infiltration showed the hub genes played an important role in AD immunity. Finally, 33 drugs targeting 10 hub genes were identified using the DrugBank database. Some of these have been clinically approved and may be useful for AD therapy. **Conclusion:** Hub genes related to disulfide levels and NAD⁺ metabolism are promising biomarkers for the diagnosis of AD. These genes may contribute to a better understanding of the pathogenesis of AD, as well as to improved drug therapy.

Keywords: Alzheimer's disease; disulfide levels; NAD⁺ metabolism; immune; drug; hub genes; diagnostic model

1. Introduction

The etiology of Alzheimer's disease (AD) is currently unclear. AD is a complex nervous system disease known to be affected by multiple factors, including neurotransmitters, immune factors, and environmental factors [1]. Accumulation of type 2 microtubule-associated (tau) protein is thought to be closely related to the decline in cognitive function in AD patients. Research has also shown that a large amount of β -amyloid protein ($A\beta$) precipitates in the brain of AD patients. This $A\beta$ accumulation can result in the formation of age-related plaques in the brain and the apoptosis of nerve cells, which is an important factor leading to AD. Although the scientific community has invested considerable resources and effort into AD research, there is still no effective prevention or treatment for this disease. Therefore, it is important to find critical molecules that could be used to develop new therapies for AD.

Nicotinamide adenine dinucleotide (NAD⁺) is the coenzyme for many dehydrogenases in the body and also connects the tricarboxylic acid cycle with the respiratory chain. Nicotinamide adenine dinucleotide (NADH) is the reduced form of NAD⁺, and their interconversion allows

mitochondria to generate energy. Beyond its role in energy metabolism, NAD⁺ is a pivotal signaling molecule essential in mediating various redox reactions, DNA maintenance and repair, gene stability, and epigenetic regulation. Decreased NAD⁺ levels have been observed in many diseases. In all organisms studied so far, from single-cell yeast to mice and humans, NAD⁺ levels have been found to decrease with age. This is because aging-induced inflammation promotes the accumulation of cyclic ADP ribohydrolyase in immune cells, hinders the cellular synthesis of nicotinamide mononucleotide (NMN), and accelerates NAD⁺ decomposition. NAD⁺ metabolism is involved in several neurodegenerative diseases [2], such as AD, Amyotrophic Lateral Sclerosis, and Parkinson's disease (PD) [3]. The NAD⁺ level in the brain of AD patients is decreased, and neuroinflammation is increased, leading to neuronal damage and cognitive impairment [4]. Restoration of NAD⁺ levels may ameliorate the various disease phenotypes by activating mitochondrial functions [5].

Under conditions of glucose starvation, high levels of SLC7A11 expression (SLC7A11^{high}) can promote cancer cell death. This is because SLC7A11^{high} cells



must rapidly reduce cystine to cysteine, which is needed to produce nicotinamide adenine dinucleotide phosphate (NADPH) from glucose and the pentose phosphate pathway (PPP). This leads to significant consumption of the cellular NADPH pool, making the cell dependent on glucose and the PPP. Therefore, when the glucose supply is limited, and oxidoreduction is insufficient, the abnormal accumulation of cysteine or other disulfide molecules in SLC7A11^{high} cells can induce disulfide stress and trigger cell death [6]. In the case of high SLC7A11 expression, glucose starvation restricts the production of NADPH by the PPP, leading to the accumulation of small molecule disulfides and cell death [6]. Other studies have confirmed that abnormal accumulation of intracellular disulfides, such as cystine, induces disulfide stress and has high cell toxicity [7,8]. Moreover, excessive disulfide levels have been found in patients with carbon monoxide (CO) poisoning [9]. Compared with the control group, the levels of disulfides in patients with early preeclampsia were significantly increased [10]. Levels of disulfide were higher in patients with type 2 diabetes mellitus compared with the control group, and a gradual increase in disulfide levels may result in the disease's severity [11].

The above findings suggest that disulfides and NAD⁺ metabolism may act together to regulate disease. We, therefore, speculated that disulfide levels and NAD⁺ metabolism may be related to AD.

To date, there have been no reports on hub genes in the disulfide levels and NAD⁺ metabolic pathways in relation to the diagnosis of AD and as possible targets for this disease. The aim of this study was, therefore, to identify hub genes for disulfide levels and NAD⁺ metabolism in AD.

2. Materials and Methods

2.1 Data Collection

The differentially expressed genes (DEGs) expression dataset was obtained from the Gene Expression Omnibus (GEO) public database in NCBI (<https://www.ncbi.nlm.nih.gov/geo/>). GSE132903 was selected for analysis of DEGs from AD patients compared with controls, which is based on platform GPL10558 and contains 97 AD samples and 98 controls [12]. Two datasets from blood, GSE63060 (145 AD and 104 controls) and GSE63061 (139 AD and 134 controls), were used as the external validation cohorts to examine the diagnostic value of hub genes. Details of the data selected are described in Table 1.

2.2 Differential Gene Expression Analysis

We used the “limma” package (<https://www.bioconductor.org/packages/release/bioc/html/limma.html>) to identify DEGs between AD and control cases. First, we removed genes with an expression value of 0 and a ratio >50%. Subsequently, we used the Voom function for data conversion and the ImFit function for multiple linear regression. Next, we computed moderated t-statistics, moderated F-statistics, and log-odds of differential expression by em-

pirical Bayes moderation of the standard errors using the eBay function. Finally, we identified DEGs with a threshold p value < 0.05, false discovery rate (FDR) < 0.05, and an absolute value of log₂-fold ≥ 0.475 .

2.3 Disulfides Levels Related Genes and NAD⁺ Metabolism-Related Genes

We screened 10 disulfide levels-related gene datasets (**Supplementary Table 1**) from the Molecular Signatures Database (MSigDB, <https://www.gsea-msigdb.org/gsea/msigdb/index.jsp>) and Kyoto Encyclopedia of Genes and Genomes (KEGG, <https://www.kegg.jp/>). After the removal of overlapping genes, 283 disulfide levels-related genes (DLRGs) were identified (**Supplementary Table 2**).

We also screened 64 NAD⁺ metabolism-related gene datasets (**Supplementary Table 1**) from the Molecular Signatures Database (MSigDB). After the removal of overlapping genes, 496 NAD⁺ metabolism-related genes (NMRGs) were identified (**Supplementary Table 2**).

2.4 WGCNA

Weighted gene co-expression network analysis (WGCNA) identifies gene sets of interest using information from thousands of genes that show the greatest changes. It performs significant correlation analysis with the phenotype and reveals interaction patterns between the genes in each sample [13]. WGCNA was used here to analyze key modules in order to understand gene association patterns between different samples. First, the median absolute deviation (MAD) of each gene was calculated, and those with a MAD < 0.5 were filtered out. Abnormal samples were removed using the R package (version 4.1.2) (R package, University of California, Los Angeles, LA, USA) “WGCNA” goodSamplesGenes method. The Pearson coefficient for the expression of any two genes in different samples was calculated. To determine whether two genes have a similar expression pattern, it is generally necessary to set a screening threshold. Those with correlation coefficients higher than the threshold are considered to have similar expressions. In this study, a correlation coefficient of >0.8 was set as the screening threshold. Subsequently, a scale-free co-expression network was constructed using WGCNA and by performing the following steps. First, both the Pearson's correlation matrices and the average linkage method were performed for all pair-wise genes. Next, the constructed weighted adjacency matrix was transformed into a topological overlap matrix (TOM) with a power of 12 to survey the network connectivity of each gene. Average linkage hierarchical clustering was performed based on TOM dissimilarity, with the threshold for minModuleSize set at 30 and the mergeCutHeight parameter set at 0.25. Genes with similar expressions were then classified into different modules, with each module depicted by a different color. Genes in gray modules were not dispensed to any module. Finally, correlations between

Table 1. The detail of selected data.

GEO accession number	Sample size (AD/control)	Platform
GSE132903 (Middle temporal gyrus)	AD = 97 HC = 98	GPL10558 Illumina HumanHT-12 V4.0 expression beadchip
GSE63060 (Blood)	AD = 145 HC = 104	GPL6947 Illumina HumanHT-12 V3.0 expression beadchip
GSE63061 (Blood)	AD = 139 HC = 134	GPL10558 Illumina HumanHT-12 V4.0 expression beadchip

CEO, Gene Expression Omnibus; AD, Alzheimer's disease; HC, Healthy control; GPL, Gene chip platform.

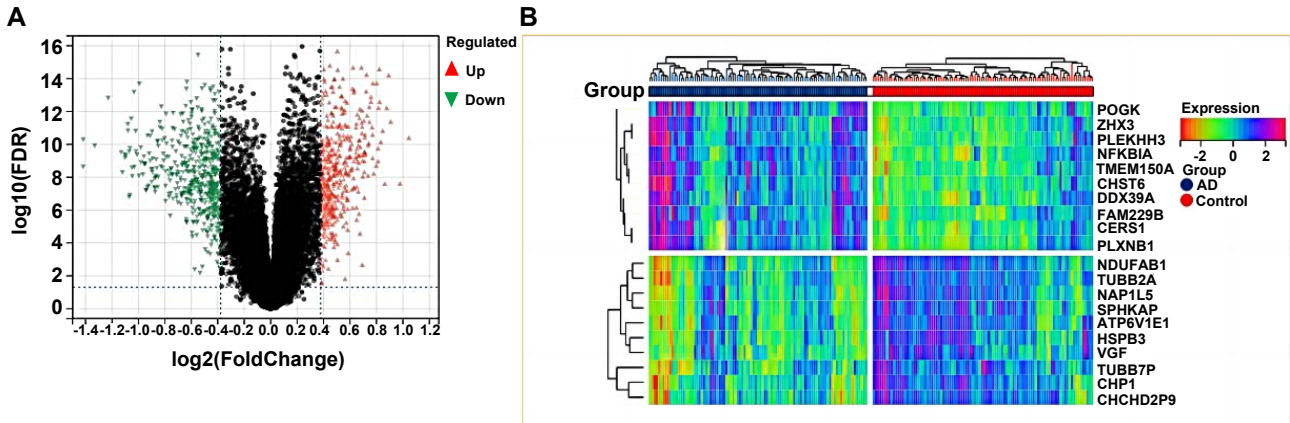


Fig. 1. Differentially expressed genes between AD and control samples. (A) The upregulated mRNAs are shown in red, and the downregulated mRNAs in green. Grey indicates no significant change. (B) The top 20 DEGs between the AD and control groups are shown as a heatmap. AD, Alzheimer's disease.

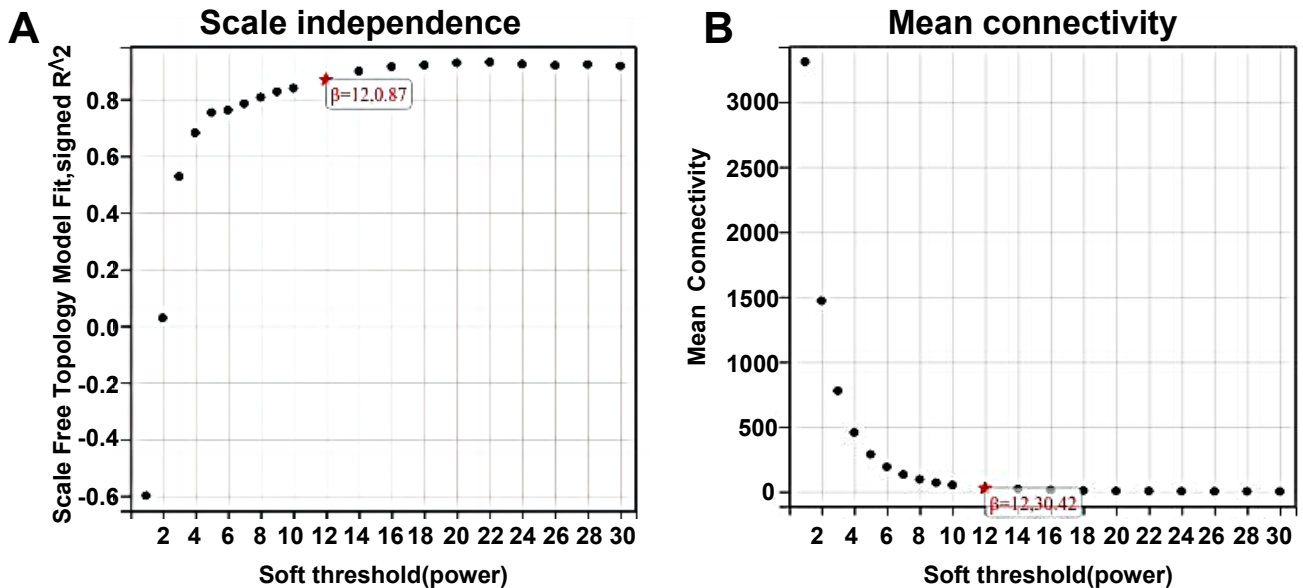


Fig. 2. Results from WGCNA based on gene expression profile. (A) The correlative scale-free topology fit indexes under the selected parameter. The horizontal axis is the soft threshold (power), while the vertical axis is the evaluation parameter of the scale-free network. The higher the value, the more the network conforms to the scale-free characteristics. (B) The correlative mean connectivity values under the selected parameter. The horizontal axis is the soft threshold (power), while the vertical axis represents the mean of all gene adjacency functions in the corresponding gene module. WGCNA, weighted gene co-expression network analysis.

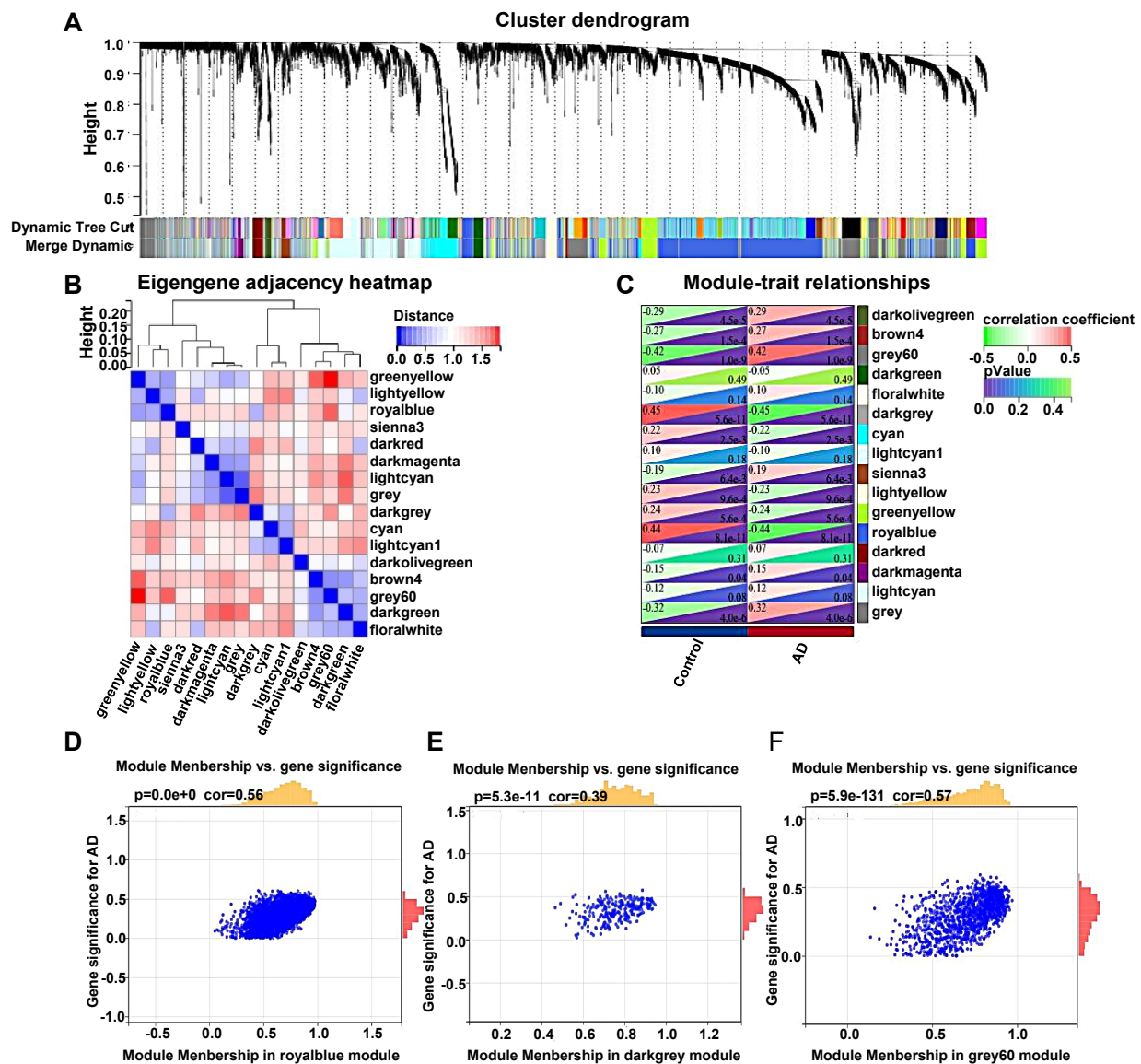


Fig. 3. Results of the WGCNA. (A) Gene cluster dendrogram. Different branches of the cluster dendrogram represent different gene modules, with different colors representing different modules. (B) Correlation heatmap between modules obtained based on the clustering of gene expression levels. The heatmap can be divided into two parts, with the upper part clustering the modules according to their eigengenes. The ordinate represents the dissimilarity of nodes, with each module represented by different colors. The abscissa and ordinate in the lower half of the figure represent different modules. Weaker correlations are more blue, while stronger correlations are more red. (C) Correlations between different modules and clinical traits. The abscissa represents different samples, while the ordinate represents different modules. The higher the absolute value of the correlation between a trait and a module, the stronger the correlation between the gene function of the trait and the module. The positive correlation is indicated by the red color, and the negative correlation is indicated by the green color. Correlations between the membership relationship and gene significance in the royal blue module (D), dark grey module (E), and grey60 module (F).

modules and phenotypes were evaluated using the module eigengenes (MEs). Modules with higher absolute values of correlation were selected as key modules for further analysis. The correlation between module feature vectors and gene expression was calculated to obtain module membership (MM). Based on the cut-off criteria of $MM > 0.08$, genes with higher connectivity in the clinically significant module were selected as hub genes.

2.5 Identification of Hub DLRGs and NMRGs

In order to identify hub genes related to both NAD⁺ metabolism and AD, the DEGs, genes in the NAD⁺ metabolism gene sets, and module genes identified by WGCNA were screened using a Venn diagram. To identify hub genes related to both disulfide levels and AD, the DEGs, genes in the disulfide levels gene sets, and module

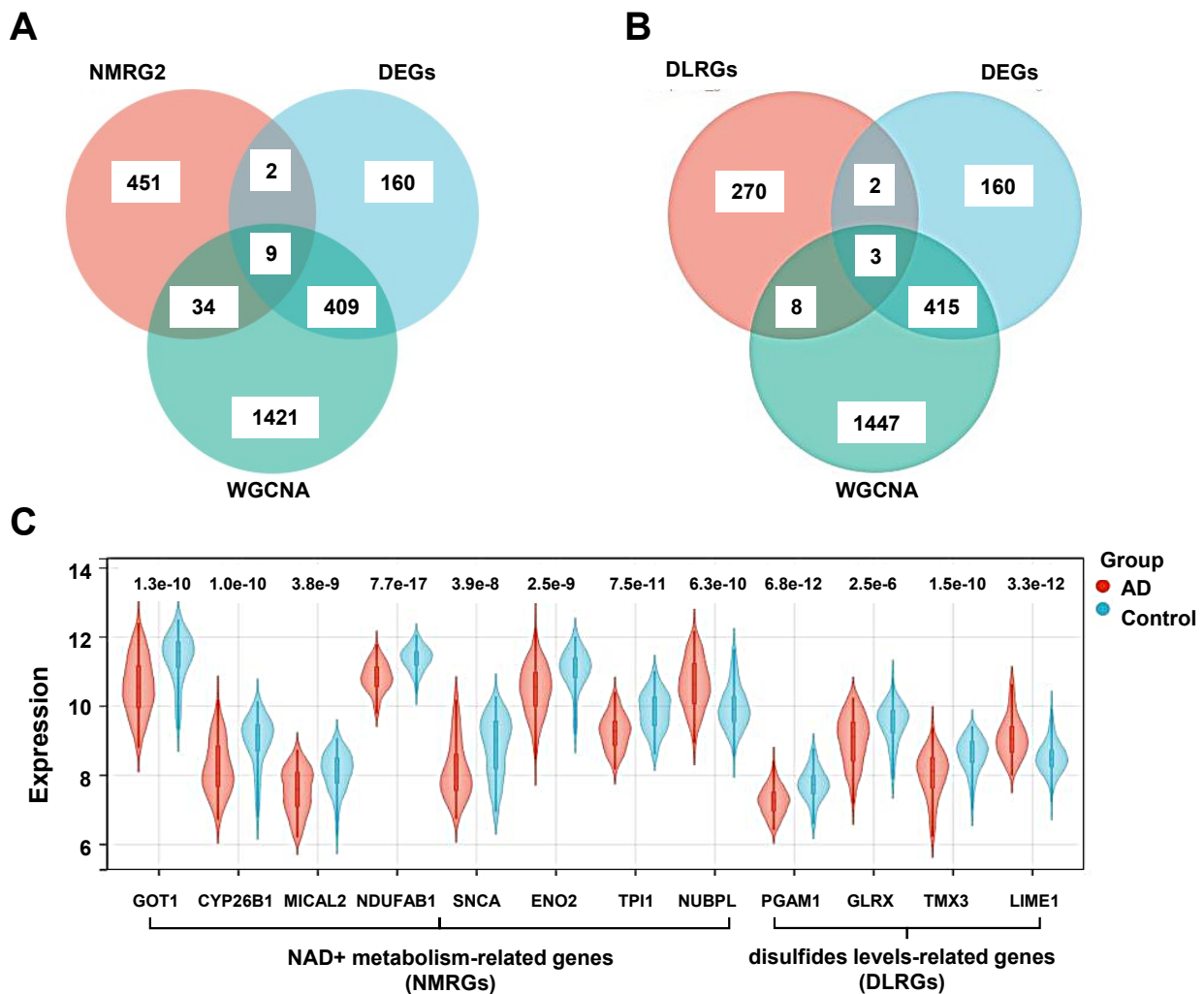


Fig. 4. Identification of NMRGs and DLRG. (A) Nine hub NMRGs were identified from the overlap of genes between DEGs, NMRGs, and genes in selected modules obtained by WGCNA. (B) Three hub DLRGs were identified from the overlap of genes between DEGs, DLRGs, and genes in selected modules obtained by WGCNA. (C) Expression of the hub DLRGs and NMRGs in the AD and control groups from GSE132903. NMRGs, NAD⁺ metabolism-related genes; DEGs, differentially expressed genes; NMRGs, NAD⁺ metabolism-related genes; DLRGs, disulfide levels-related genes.

genes identified by WGCNA were also screened using a Venn diagram. Differences in the expression of hub NMRGs and DLRGs between AD and control samples were displayed by violin plot.

2.6 Pathway Analysis of Hub DLRGs and NMRGs

Pathway analysis was conducted to explore the mechanism by which hub NMRGs and DLRGs could be associated with AD. Gene set enrichment analysis (GSEA) reveals the distribution trend of each gene in the gene table sorted by phenotype correlation, thereby allowing evaluation of the effect of synergistic changes in genes on phenotypic changes. Samples were divided into low- and high-expression groups according to the average expression level of hub NMRGs and DLRGs. Background gene sets were downloaded from the Molecular Signatures Database (<http://www.gsea-msigdb.org/gsea/msigdb/index.jsp>) to evalu-

ate the relevant pathways and molecular mechanisms involving hub NMRGs and DLRGs. The thresholds for selecting targets were $p < 0.05$ and $FDR < 0.25$.

2.7 Construction of a Diagnostic Model

Cox's proportional hazards regression model (Cox regression model) is used mainly for the prognostic analysis of tumors and other chronic diseases but can also be used to explore etiology in cohort studies. It is widely used in clinical practice, with the results obtained often having direct clinical applications. Cox analysis plays a crucial role in the clinical diagnosis of AD. In this study, expression levels for the 12 hub DLRGs and NMRGs were first adjusted for covariates such as sex and age (**Supplementary Tables 3–5**). The “survival” package in R (version 4.1.2) (R package, University of California, Los Angeles, LA, USA) was then used to integrate survival time, survival status, and ex-

pression levels for the 12 hub DLRGs and NMRGs. Cox analysis was used to evaluate the prognostic significance of the 12 hub genes in samples from GSE132903, GSE63060, and GSE63061 and to obtain the RiskScore. Diagnostic receiver operating characteristic curve (ROC) analysis was performed using the roc function of “pROC” packages (version 1.17.0.1) (<https://www.rdocumentation.org/packages/pROC/versions/1.17.0.1>) in R software. The ci function of the “pROC” package in R software was then used to evaluate the area under the ROC curve (AUC) and the confidence intervals. Next, the diagnostic ROC model was applied to samples from GSE132903, GSE63060, and GSE63061 using only demographic information such as sex and age. Finally, the log-rank test was performed to compare the two models and thus determine the additional value gained from the 12 hub genes.

2.8 Investigation of Immune Cell Type Fractions, Immune-Related Factors, and MHCs

The infiltration of immunocytes in AD and control samples from GSE132903 was evaluated using CIBERSORT (<https://cibersortx.stanford.edu/>) based on gene expression data. Spearman correlation analysis was performed between the 12 hub DLRGs and NMRGs and various immune factors, immune infiltration, and major histocompatibility complex (MHC) using the “psych” package in R software (version 4.1.2) (R package, University of California, Los Angeles, LA, USA). Immune factors and MHC were downloaded from the TISIDB database (<http://cis.hku.hk/TISIDB/>) [14]. These included 24 immunoinhibitors, 46 immuno-stimulators, 41 chemokines, and 21 MHCs.

2.9 Identification of Targeted Drugs for Hub DLRGs and NMRGs in the DrugBank

We searched the DrugBank database (<https://go.drugbank.com>) (University of Alberta, Edmonton, Alberta, Canada) [15] for possible targeted drugs against the hub genes. The DrugBank database integrates bioinformatics and chemical informatics to provide detailed drug data, target information, and comprehensive information on their mechanism of action, including drug chemistry, pharmacology, pharmacokinetics and interactions. The latest version of DrugBank (5.1.10) was released on January 4, 2023, and contained 15,664 drug entries, including 2742 approved small molecule drugs, 1584 approved biologic agents (proteins, peptides, vaccines, and allergens), 134 nutritional products, and 6720 experimental drugs.

3. Results

3.1 Identification of DEGs

To investigate the changes in gene expression that occur in AD, we screened for DEGs between the AD and control groups. DEGs are displayed in a volcano plot in Fig. 1A, and the top 20 DEGs are shown in a heatmap in

Fig. 1B. Using a threshold of $p < 0.05$ and an absolute value of ≥ 0.475 for log 2-fold, a total of 580 DEGs were identified in GSE132903 (**Supplementary Table 6**).

3.2 Identification of Hub DLRGs and NMRGs

We next performed WGCNA of these DEGs to identify those that play a significant role in the pathological mechanism of AD. The parameters selected for WGCNA were a soft threshold of 12, a scale independence of 0.87, and an average connectivity of 30.42 (Fig. 2A,B). With threshold values of 0.25 for mergeCutHeight and 30 for minModuleSize, 16 co-expression modules were acquired (Fig. 3A,B). Correlations between each module and AD features were then analyzed (Fig. 3C). The strongest positive correlation with AD was seen with the grey60 module ($r = 0.42$, $p = 1.0 \times 10^{-9}$) (Fig. 3D). The strongest negative correlation was with the dark gray module ($r = -0.45$, $p = 5.6 \times 10^{-11}$) (Fig. 3E), followed by the royal blue module ($r = -0.44$, $p = 8.1 \times 10^{-11}$) (Fig. 3F). The 1873 genes contained within the grey60, dark grey and royal blue modules were selected for further analysis. Nine hub genes related to NAD⁺ metabolism and AD were identified as overlapping genes between the 580 DEGs, 496 NMRGs, and 1873 genes in the selected modules (Fig. 4A). Furthermore, 3 hub genes related to disulfides levels and AD were identified as overlapping genes between the 580 DEGs, 283 DLRGs, and 1873 genes in the selected modules (Fig. 4B). Violin plots showed that expression of *NUBPL* and *LIME1* was upregulated in AD from GSE132903, whereas expression of the other 10 genes (*GOT1*, *CYP26B1*, *MICAL2*, *NDU-FAB1*, *SNCA*, *ENO2*, *TPII*, *PGAM1*, *GLRX* and *TMX3*) was downregulated compared to the controls (Fig. 4C).

3.3 Pathway Analysis

Pathway analysis of the hub DLRGs and NMRGs was conducted to study possible biological mechanisms relating to AD. The putative functions of the 12 hub DLRGs and NMRGs in AD were analyzed by GSEA (Fig. 5A–L).

3.4 Establishment and Validation of a Diagnostic Model for AD

A predictive model was constructed to test the diagnostic value of the hub genes. Using stepwise regression analysis, the 3 hub DLRGs and 9 hub NMRGs were selected to build an optimal model. The AUC of this predictive model was 0.935 in brain tissue samples, suggesting the 12 hub DLRGs and NMRGs had good diagnostic performance (Fig. 6A). The diagnostic value of the hub genes was next examined in blood samples. Using the model, the AUCs obtained in the GSE63061 and GSE63060 cohorts were 0.740 and 0.705, respectively (Fig. 6B,C). The higher AUC observed in brain samples indicates the diagnostic superiority of this tissue source. However, because of the difficulty in obtaining brain tissue, models that produce good results using blood samples may be helpful for the early di-

agnosis of AD patients. In order to confirm the added value of these genes, diagnostic ROC analysis of the GSE132903, GSE63060 and GSE63061 cohorts was performed using a model containing only demographic factors such as sex and age (Fig. 6D,E,F).

To estimate the additional diagnostic value provided by the 12 hub genes, ROC models that included only demographic factors such as sex and age were used for the GSE132903, GSE63060, and GSE63061 cohorts. The AUC value of 0.504 obtained for the GSE132903 cohort was significantly lower ($p < 0.0001$) than using the model containing the 12 hub DLRGs and NMRGs. Similarly, the AUC values for GSE63060 (0.642) and GSE63061 (0.630) were both significantly lower ($p < 0.0001$).

3.5 Investigation of Immune Cell Type Fractions, Immune-Related Factors and MHC

We next analyzed the infiltration of immunocytes in AD by evaluating the proportion of 22 immune cell types in AD and control samples using the CIBERSORT algorithm (Fig. 7A). Correlation analysis showed that macrophages M2 and neutrophils had a synergistic effect. Furthermore, macrophages M0 and macrophages M2 showed the strongest competitive effect (Fig. 7B). A violin plot was used to show differences in the immune infiltration score between AD and control groups (Fig. 7C). The AD group had significantly higher proportions of B cells naive ($p = 0.02$) and neutrophils ($p = 0.01$) than the control group, whereas the proportions of macrophages M1 ($p = 1.5 \times 10^{-3}$), T cells CD4 memory ($p = 0.01$) and T cells gamma delta ($p = 0.05$) were lower in AD than in controls. Next, we investigated possible correlations between the 12 hub DLRGs and NMRGs and the infiltration with immunocytes and immune factors. Dendritic cells activated and T cells follicular helper showed significant negative correlations with *NUBPL* and *LIME1*, whereas macrophages M1, plasma cells, and T cells CD4 naive were positively correlated with *NUBPL* and *LIME1*. Dendritic cells activated and T cells follicular helper correlated positively with the other down-regulated genes (*GOT1*, *CYP26B1*, *MICAL2*, *NDUFAB1*, *SNCA*, *ENO2*, *TPH1*, *PGAMI*, *GLRX* and *TMX3*), whereas macrophages M1, plasma cells and T cells CD4 naive were negatively correlated with these genes (Fig. 8A). The correlation of the 12 hub DLRGs and NMRGs with different immune factors (immune-inhibitors, immune-stimulators, and chemokines) and with MHC are shown as heatmaps in Fig. 8B–E. The above results indicate that the 12 hub DLRGs and NMRGs may be closely related to the immune microenvironment.

3.6 Drugs Predicted to Target the Hub DLRGs and NMRGs

Based on drug and target information from the DrugBank database, we identified 33 drugs targeting 10 hub DLRGs and NMRGs (Fig. 9). Of these, 17 have been approved, 2 are investigational, and 12 are experimen-

tal. Adapalene (DB00210), an inhibitor of *GOT1*, is used to treat acne vulgaris. Molecular docking has shown that adapalene coordinates with *GOT1* at its allosteric site with low binding energy. Knockout of *GOT1* reduces cell sensitivity to the anti-proliferative effect of adapalene. This drug is reported to inhibit the growth of ES-2 ovarian cancer cells by targeting glutamic-oxaloacetic transaminase 1 (*GOT1*). Copper (DB09130) targets *SCNA*, *GOT1*, *MICAL2*, *PGAMI*, and *TMX3* and is used for total parenteral nutrition supplementation and intrauterine device contraception. The effect of low-dose copper on *PGAMI* was tested by 2-dimensional fluorescence difference gel electrophoresis coupled with matrix-assisted laser desorption/ionization time-of-flight mass spectrometry (MALDI-TOF-MS/MS). This showed that copper significantly down-regulates the expression of *PGAMI* [16]. Pyridoxal phosphate (DB00114) is an activator of *GOT1* and is used for nutritional supplementation. *In silico* docking analysis suggests that *GOT1* inhibitor competes for binding to the pyridoxal phosphate cofactor site of *GOT1*. Mutational studies have revealed the relationship between pyridoxal phosphate binding and the thermal stability of *GOT1* [16]. Zinc chloride (DB14533) binds to *TPH1* and *TMX3* and is used to maintain zinc serum levels and prevent deficiency syndromes. Zinc sulfate (DB14548) also binds to *TPH1* and *TMX3* and is used for zinc supplementation in parenteral nutrition. Arteminol (DB11638) targets *TMX3*, *PGAMI*, and *TPH1* and is used to treat uncomplicated plasmodium falciparum infection. Aspartic acid (DB00128) targets *GOT1* and is used to enhance exercise performance. Cysteine (DB00151) targets *GOT1* and is used to prevent liver and kidney damage associated with acetaminophen overdose. Glutamic acid (DB00142) targets *GOT1* and is used to improve mental capacity. Vitamin A (DB00162) is a substrate inducer of *CYP26B1* and is used to treat vitamin A deficiency. Tretinoin (DB00755) is a substrate of *CYP26B1* and is used to induce remission from acute promyelocytic leukemia in adult patients and pediatric patients older than 1 year. Human calcitonin (DB06773) targets *MICAL2* and is used to treat Paget's disease. NADH (DB00157) targets NADH: ubiquinone oxidoreductase subunit AB1 (*NDUFAB1*) and is used to treat many neurodegenerative diseases. Zinc (DB01593) targets *TPH1* and *TMX3* and is used to treat and prevent zinc deficiency and its consequences. Zinc acetate (DB14487) also targets *TPH1* and *TMX3* and is used to treat and prevent zinc deficiency and its consequences, to boost the immune system, and to treat the common cold and recurrent ear infections. Glutathione (DB00143) targets *GLRX* and is used for nutritional supplementation and the treatment of dietary deficiency or imbalance.

4. Discussion

Nicotinamide adenine dinucleotide consists of oxidized (NAD⁺) and reduced (NADH) forms. NAD⁺ is a ma-

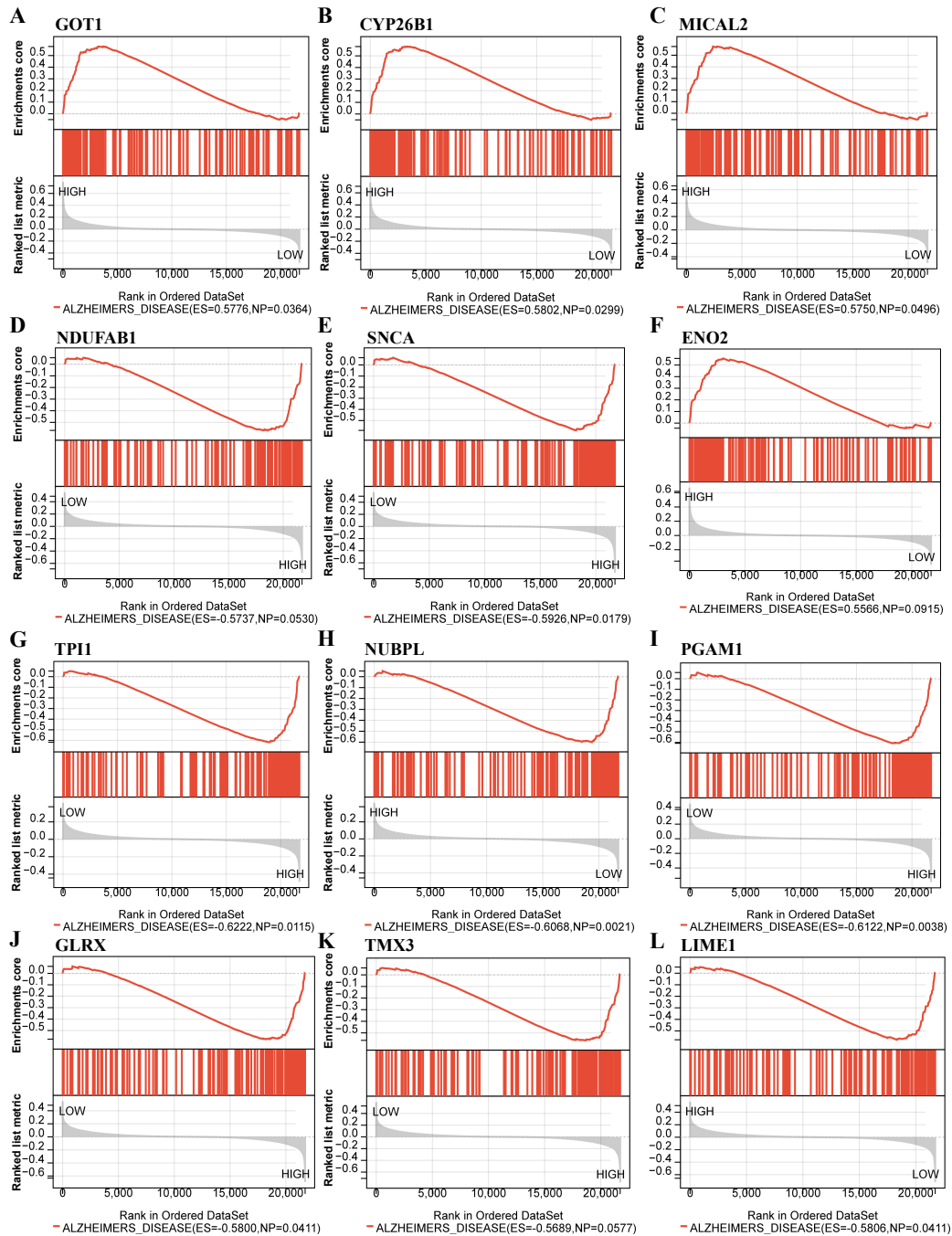


Fig. 5. GSEA was used to analyze the putative functions of the 12 hub DLRGs and NMRGs in AD. (A) GOT1, (B) CYP26B1, (C) MICAL2, (D) NDUFAB1, (E) SNCA, (F) ENO2, (G) TPI1, (H) NUBPL, (I) PGAM1, (J) GLRX, (K)TMX3, and (L) LIME1. GSEA, Gene set enrichment analysis; GOT1, glutamic-oxaloacetic transaminase 1; CYP26B1, cytochrome P450 family 26 subfamily B member 1; MICAL2, microtubule associated monooxygenase, calponin and LIM domain containing 2; NDUFAB1, NADH: ubiquinone oxidoreductase subunit AB1; SNCA, synuclein alpha; ENO2, enolase 2; TPI1, triosephosphate isomerase 1; NUBPL, NUBP iron-sulfur cluster assembly factor, mitochondrial; PGAM1, phosphoglycerate mutase 1; GLRX, glutaredoxin; TMX3, thioredoxin related transmembrane protein 3; LIME1, Lck interacting transmembrane adaptor 1.

major coenzyme in the tricarboxylic acid cycle and can influence many key cell functions, including DNA repair, chromatin remodeling, immune cell function, and cell aging. Aging is closely related to most neurodegenerative diseases and is associated with decreased cellular levels of NAD⁺ in

the brain [17]. Depletion of NAD⁺ has been found in several models of accelerated aging that exhibit certain characteristics of neurodegenerative disease [5]. Recent studies have also found that high levels of accumulated disulfides result in abnormal disulfide binding between actin cy-

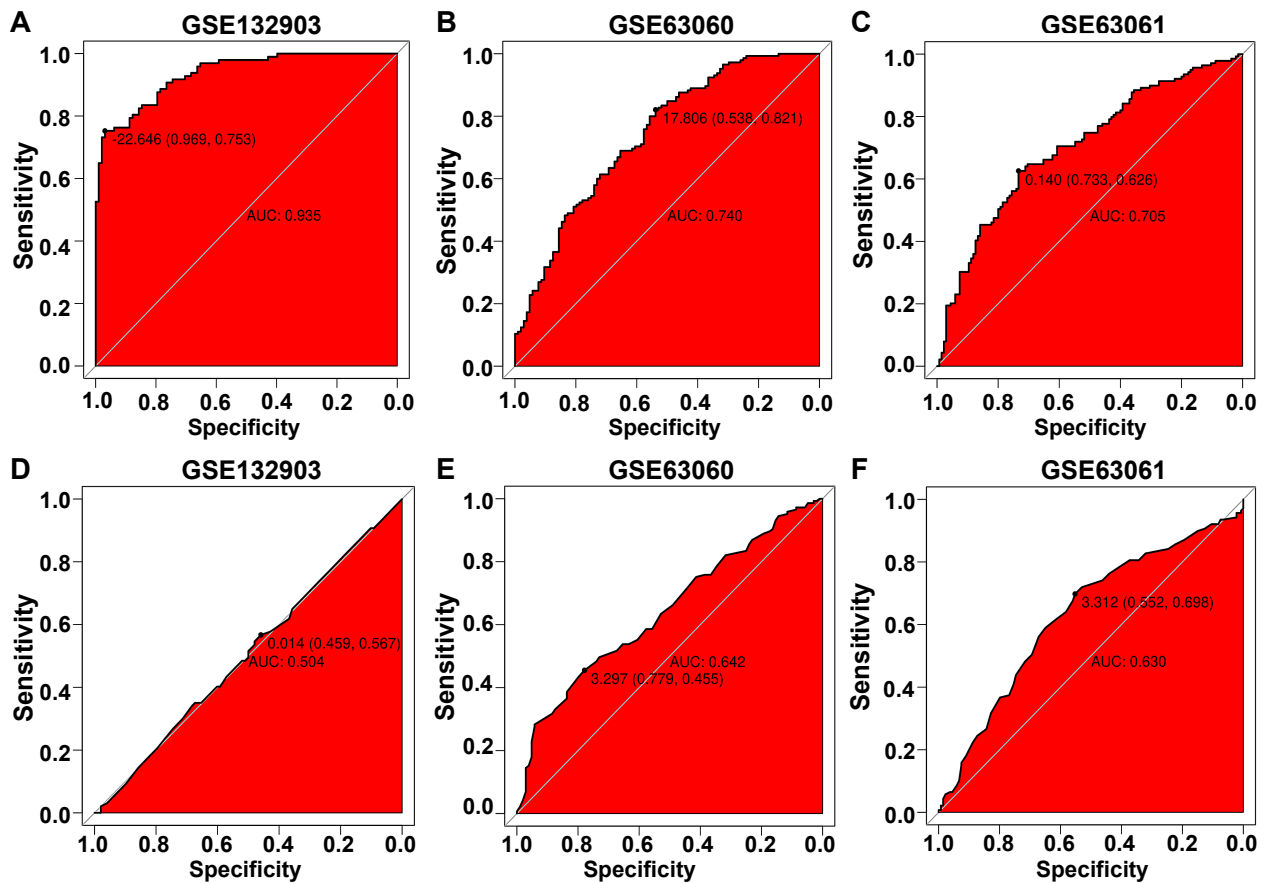


Fig. 6. Diagnostic ROC and relevant AUC values for the three AD cohorts. Diagnostic ROC analysis of the (A) GSE132903, (B) GSE63060, and (C) GSE63061 cohorts using a model containing expression levels for the 12 hub DLRGs and NMRGs, and adjusted for covariates such as sex and age. Diagnostic ROC analysis of the (D) GSE132903, (E) GSE63060, and (F) GSE63061 cohorts using a model containing only demographic factors such as sex and age. ROC, receiver operating characteristic; AUC, area under the curve.

toskeleton proteins, eventually leading to a collapse of the actin network and cell death [6]. Reduced actin is significantly correlated with cognitive impairment and with $A\beta$ protein levels in AD. Based on the above observations, a correlation between abnormal disulfide levels and NAD^+ metabolism and AD disease has been proposed.

In the current study, 3 genes related to AD and disulfide levels were identified (*GLRX*, *TMX3*, and *LIME1*), as well as 9 genes related to AD and NAD^+ metabolism (*GOT1*, *CYP26B1*, *MICAL2*, *NDUFAB1*, *SNCA*, *ENO2*, *TP11*, *NUBPL* and *PGAM1*). Pathway analysis revealed these genes were involved in AD. Furthermore, Gene Ontology (GO) enrichment analysis showed they were involved in oxidation-reduction and NADH regeneration processes to regulate the function of mitochondria. Abnormal expression of these genes leads to dysfunction of mitochondria and the production of reactive oxygen species (ROS) in the cell microenvironment [18]. Excess ROS can damage biological cell macromolecules such as proteins, nucleic acids, and lipids. This affects their normal physiological functions, eventually leading to necrosis and apoptosis and accelerating the occurrence and development of AD [19].

As a metabolic cofactor, NAD^+ plays a crucial role in mitochondrial function. Wu *et al.* [20] proposed that ROS formation induced by $A\beta_{25-35}$ in primary rat cortical neurons was eliminated by NAD^+ .

We constructed a diagnostic model to determine whether the 12 hub DLRGs and NMRGs identified in AD patients could predict prognosis in clinical applications. The AUC for this predictive model was 0.935 using brain tissue samples and 0.740 and 0.705 using blood samples, indicating good diagnostic performance with the 12 hub DLRGs and NMRGs. The blood sample model allows clinical diagnosis of AD patients in cases where it is difficult to obtain brain tissue. *GOT1* is considered to be a key metabolic gene related to AD [21] and codes for glutamic oxaloacetic transaminase in the cytoplasm. This gene was reported to be downregulated in the elderly population and AD patients [22]. Retinoic acid (RA) is metabolized into an inactive form by *CYP26B1*, which is a member of the cytochrome P450 enzyme family. Decreased *CYP26B1* levels have been reported in a mouse model of AD [23]. *NDUFAB1* is a novel molecule that enhances mitochondrial metabolism and is associated with signaling pathways for

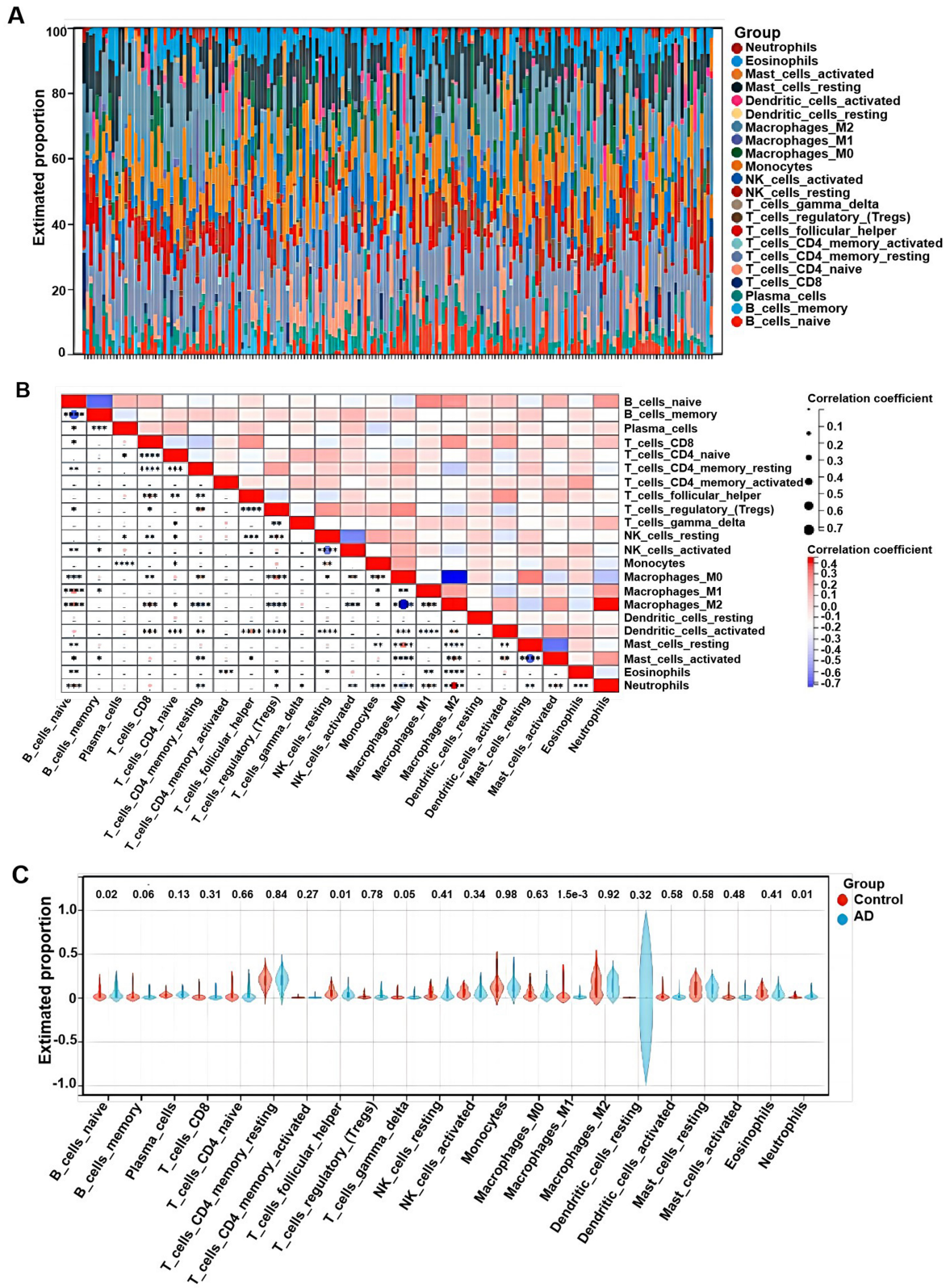


Fig. 7. Comparison of immunocyte infiltration between AD and control samples. (A) The percentage of 22 immune cell types in each sample. (B) Co-expression patterns between the different types of immune cells. Red: positive correlation; Blue: negative correlation. (C) Immune infiltration score in the AD and control samples. * represents the correlation coefficient bigger than 0.1 but less than 0.2. ** represents the correlation coefficient bigger than 0.2 but less than 0.35. *** represents the correlation coefficient bigger than 0.35 but less than 0.4. **** represents the correlation coefficient bigger than 0.4.

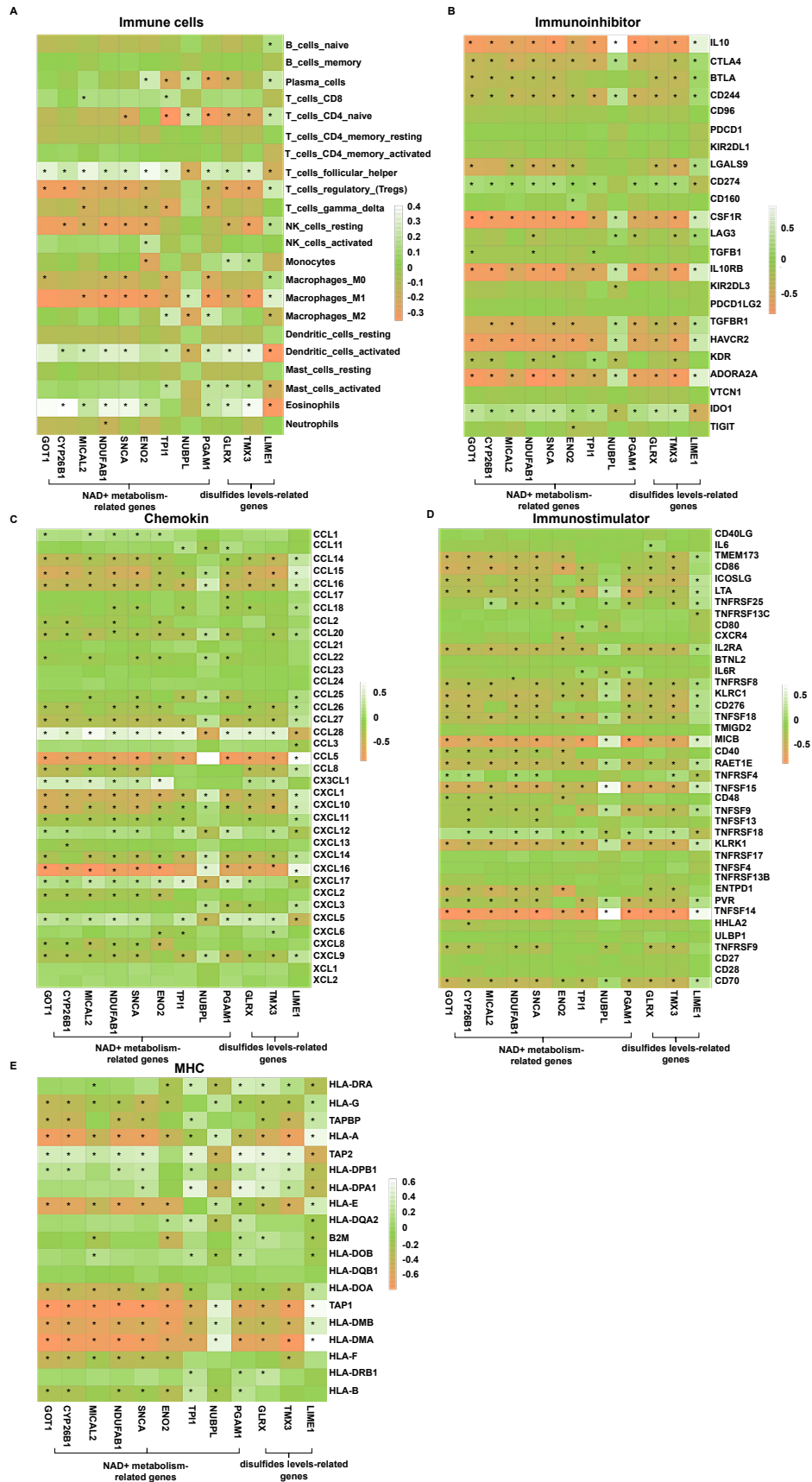


Fig. 8. Spearman correlation analysis of the 12 hub DLRGs and NMRGs with (A) immune cells, (B) immune inhibitors, (C) chemokines, (D) immune stimulators, and (E) MHC. Green: positive correlation; Red: negative correlation; *, significant difference. MHC, major histocompatibility complex.

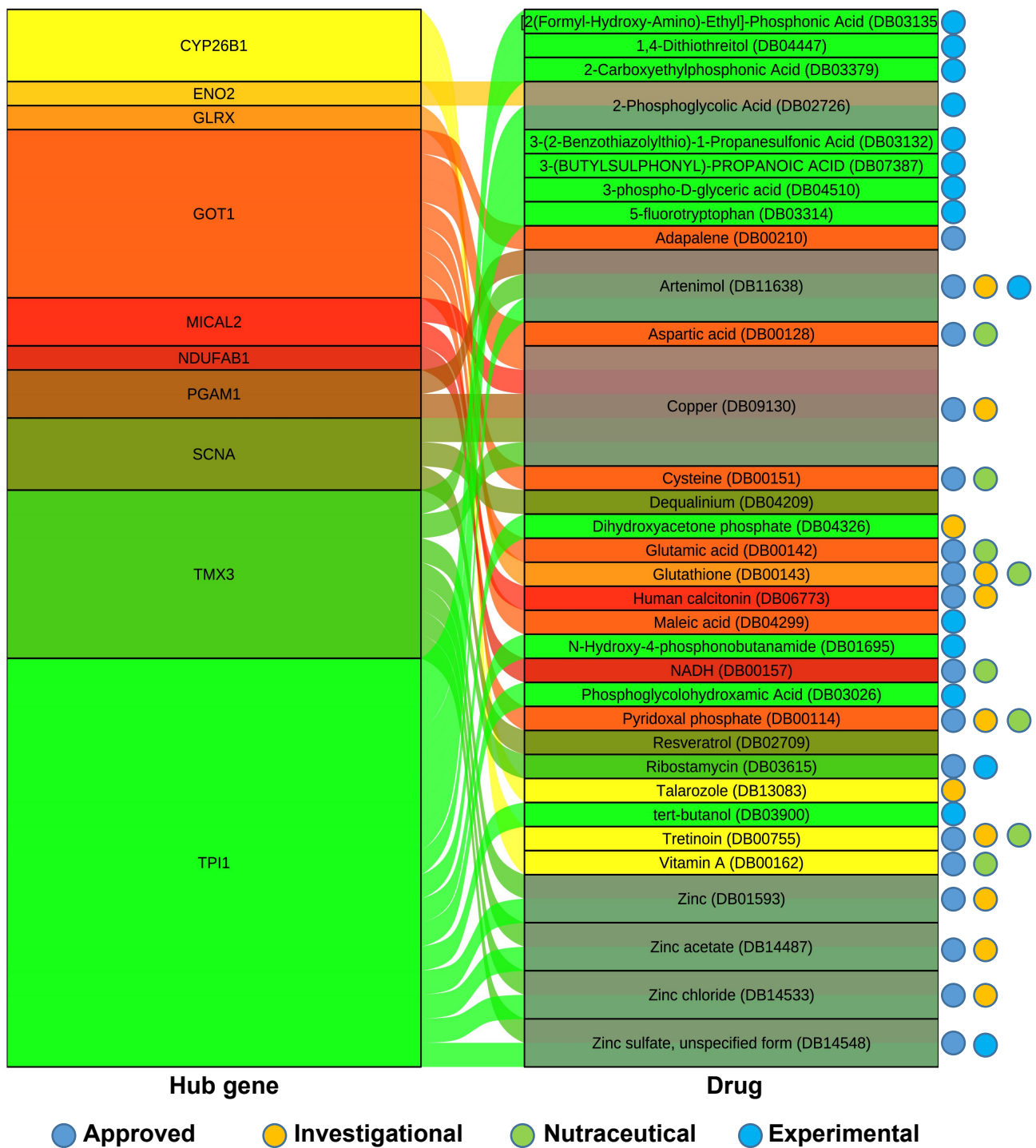


Fig. 9. Drugs targeting 10 hub DLRGs and NMRGs, as identified in the DrugBank database. The drug status (approved, investigational, nutraceutical, or experimental) is indicated by the colored circles.

oxidative phosphorylation [24]. Musculoskeletal aging and AD show an imbalance in the expression of *NDUFAB1* [25]. Synuclein alpha (*SNCA*) is thought to be associated with memory, learning abilities, and neurodegenerative diseases [26]. Single nucleotide polymorphisms in *SNCA*, such as rs3857059, rs2583988, and rs10516846, have been associated with a higher risk of AD [27,28]. The enolase *ENO2*

is expressed mainly in neurons of the whole neuraxis [29] and is regarded as a diagnostic marker for AD [30].

The enzyme triose phosphate isomerase (*TPI*) catalyzes the reversible conversion between dihydroxyacetone phosphate isomers and glyceraldehyde 3-phosphate. Deletion of *TPI* has been shown to induce neurologic abnormalities, and *TPI* could also be a hub gene that participates in

the molecular pathogenesis of AD [31,32]. Phosphoglycerate mutase 1 (PGAM1) is a major enzyme in the glycolysis pathway and is very sensitive to oxidative stress. PGAM1 can inhibit glycolysis and is prone to oxidation in neurological diseases such as AD [33,34]. Glutaredoxin (GLRX) is a major member of the thiol/disulfide bond oxidoreductase family that catalyzes redox reactions between glutathione (GSH) and protein disulfide bonds. Abnormalities in the aggregation, structure, and function of actin have been found to affect dendritic spines in AD [35]. Overexpression of *GLRX1* can rescue these deficits by restoring F-actin dynamics in dendritic spines. Another actin modulator, LIM domain kinase 1 (LIMK1), was also reported to be involved in the assembly and decomposition of F-actin in AD [36]. Thioredoxin related transmembrane protein 3 (TMX3) is a member of the disulfide isomerase family of endoplasmic reticulum proteins. Decreased expression of *TMX3* was reported in association with mutant huntingtin protein [37]. However, further research is needed to determine whether upregulation of *TMX3* expression in the brain could improve neurodegeneration.

The pathogenesis of AD is not limited to neuronal regions, with many brain immune cells such as astrocytes, macrophages (microglia in the brain), and peripheral infiltrating immune cells also being involved. The infiltration of immunocytes and immune factors was investigated in the present study, with box plots used to show the marked differences in immunocytes between AD and control groups. The level of infiltration by naive B cells was higher in the AD group, in accordance with a previous study [38]. Neutrophils were also more common in the brain of AD patients, with these cells usually being the first responders to inflammation [39]. Neuroinflammation is a significant factor in the pathogenesis and development of AD. An increased level of CD11b integrin was reported in the peripheral blood neutrophils of AD patients [40]. In addition, neutrophils have been shown to accumulate in AD and have been implicated in its pathology and associated cognitive impairment [41]. Moreover, the depletion of neutrophils resulted in decreased levels of phosphorylated tau in a mouse model of AD. In the current study, significant correlations were found between 12 hub DLRGs and NMRGs and different immune factors and are shown using heatmaps. Correlations between AD and immune, inflammatory, and cell death pathways were also confirmed. Immune signaling and cell death pathways ultimately cause the release of cytokines and chemokines that participate in pro-inflammatory and anti-inflammatory processes, neuron injury, and microglial effects on $A\beta$ deposition. The colony-stimulating factor 1 receptor (CSF1R) is a member of the type III receptor tyrosine kinase family that plays a major role in microglial homeostasis, neurogenesis, and neuronal survival [42]. *CSF1R* mutation has been associated with the clinical phenotype of AD. In addition, various *CSF1R* genetic variants (p.P54Q, p.L536V, p.L868R,

p.Q691H, and p.H703Y) have been associated with the risk of AD [43]. An inhibitor of *CSF1R* has been reported to eliminate microglia, reduce the accumulation of $A\beta$, reduce neuritic and synaptic damage, and improve cognition in different AD-related mouse models [44].

Besides cytokines, chemokines also enhance local inflammation in AD by regulating the migration of microglia to the neuroinflammatory region. C-X3-C motif chemokine ligand 1 (CX3CL1) is the only member of the chemokine CX3C family and is commonly present in the entire brain, particularly in neural cells. The levels of CX3CL1 were reported to be significantly reduced in the hippocampus, frontal cortex, and cerebrospinal fluid of AD patients compared to healthy controls [45]. Unlike other chemokines, CX3CL1 only interacts with the C-X3-C motif chemokine receptor 1 (CX3CR1) expressed on microglia and hence plays a crucial role in neuron-microglial communication [46]. It has been suggested that abnormal CX3CL1/CX3CR1 signaling could affect AD pathogenesis and progression [47]. Chemokine (C-X-C motif) ligand 1 (CXCL1) is a significant member of the CXC chemokine family and binds to the CXCR2 receptor. CXCL1 is found in various cell types, including neutrophils and oligodendrocytes, and may have important pro-nociceptive effects through direct effects on sensory neurons. CXCL1 has been shown to activate caspase-3-dependent tau proteins, resulting in the aberrant extracellular distribution of these abnormal tau proteins [48].

We identified 33 drugs in the DrugBank database that target 10 of the hub genes. Copper is an essential biomolecule in human physiology and plays an important role against oxidative stress [49]. Disruptions in the metabolism and distribution of copper have been reported in AD patients. An indicator of abnormal copper metabolism is increased levels of non-ceruloplasmin copper, which has been associated with a higher risk of AD [50]. Copper (DB09130) is considered to be a potential therapeutic target for AD due to its redox ability. Consequently, a large number of ligands have been developed to disrupt the $A\beta$ -copper interaction and thus reduce copper-related toxicity [51]. Pyridoxal phosphate is a cofactor for various enzyme reactions involved in protein, glucose, and lipid metabolism and has been associated with the stabilization of protein and neurotransmitter biosynthesis. The administration of pyridoxal phosphate (DB00114) markedly reduces $A\beta_{25-35}$ -induced production of malondialdehyde and nitric oxide in the brain [52]. Pyridoxal phosphate can inhibit lipid peroxidation and eliminate nitric oxide (NO), thereby protecting against $A\beta_{25-35}$ -induced cognitive impairment. Cysteine is a reducing agent that weakens protein structures by altering disulfide bonds between and within protein molecules. Supplementation with cysteine (DB00151) may promote the synthesis of GOT1 in the brain, thus helping to prevent AD [53]. A previous *in vivo* study showed that vitamin A deficiency can lead to the accumulation of $A\beta$ [54]. The

administration of nutritional vitamin A (DB00162) in pre-clinical intervention studies using elderly rats and mice was found to strengthen synaptic plasticity, improve hippocampal neurogenesis, and rescue multiple memory deficits [55]. Recent work has shown that administering vitamin A can help prevent AD neuropathy in males [56]. Calcitonin (DB06773) is a 32 amino acid peptide hormone that can act as a nerve regulator and/or neurotransmitter in the central nervous system [57]. NADH is one of the core electron donors with a significant role in mitochondrial oxidative phosphorylation. It is used to move electrons along the electron transfer chain during the production of ATP [58]. NADH (DB00157) could, therefore, be a useful neuroprotective therapy and is currently undergoing clinical trials for AD. An open-label study on 17 AD patients showed that 10 mg/day of NADH intake for 8–12 weeks led to improved cognitive function [59]. Zinc deficiency is a worldwide problem. AD patients have lower serum zinc levels compared to healthy elderly controls, suggesting a latent role for disordered zinc homeostasis in this disease [60]. Zinc (DB01593) therapy has proven to be effective in AD clinical tests, with improved cognitive performance possibly due to a latent effect from reduced non-ceruloplasmin copper [61].

5. Conclusion

In conclusion, we identified 12 hub genes that link disulfide levels and NAD⁺ metabolism with AD. The pathways enriched by these genes may help to shed light on the mechanism of AD pathogenesis. However, further experiments are needed to confirm the functions of these hub genes. We built a diagnostic model for the diagnosis of AD based on the expression levels for the 12 DLRGs and NMRGs in brain and blood samples. Moreover, these genes were found to be associated with distinct immune factors, indicating they play a major role in the immune microenvironment. Our study also predicted drugs that could be used to target the hub genes, thus providing valuable insights for the treatment of AD.

Availability of Data and Materials

All the data supporting the results of this study are included in the manuscript and the Supplementary Documents.

Author Contributions

LS and YW designed the study. LS, YZ and YW performed the data analysis. YW and LS wrote the manuscript. HW collected and sort references, designed and drew the figures and tables. All authors contributed to editorial changes in the manuscript. All authors read and approved the final manuscript. All authors have participated sufficiently in the work and agreed to be accountable for all aspects of the work.

Ethics Approval and Consent to Participate

Not applicable.

Acknowledgment

Not applicable.

Funding

This work was supported by excellent youth fund for basic scientific research projects of Hebei North University (JYT2023002), youth fund for basic scientific research projects of Hebei North University (JYT2022008) and the Project of Hebei North University (H2022405030), China.

Conflict of Interest

The authors declare no conflict of interest.

Supplementary Material

Supplementary material associated with this article can be found, in the online version, at <https://doi.org/10.31083/j.jin2304085>.

References

- [1] Gu X, Lai D, Liu S, Chen K, Zhang P, Chen B, *et al.* Hub Genes, Diagnostic Model, and Predicted Drugs Related to Iron Metabolism in Alzheimer's Disease. *Frontiers in Aging Neuroscience*. 2022; 14: 949083.
- [2] Zheng M, Schultz MB, Sinclair DA. NAD⁺ in COVID-19 and viral infections. *Trends in Immunology*. 2022; 43: 283–295.
- [3] Li C, Zhu Y, Chen W, Li M, Yang M, Shen Z, *et al.* Circulating NAD⁺ Metabolism-Derived Genes Unveils Prognostic and Peripheral Immune Infiltration in Amyotrophic Lateral Sclerosis. *Frontiers in Cell and Developmental Biology*. 2022; 10: 831273.
- [4] Hou Y, Wei Y, Lautrup S, Yang B, Wang Y, Cordonnier S, *et al.* NAD⁺ supplementation reduces neuroinflammation and cell senescence in a transgenic mouse model of Alzheimer's disease via cGAS-STING. *Proceedings of the National Academy of Sciences of the United States of America*. 2021; 118: e2011226118.
- [5] Hikosaka K, Yaku K, Okabe K, Nakagawa T. Implications of NAD metabolism in pathophysiology and therapeutics for neurodegenerative diseases. *Nutritional Neuroscience*. 2021; 24: 371–383.
- [6] Liu X, Nie L, Zhang Y, Yan Y, Wang C, Colic M, *et al.* Actin cytoskeleton vulnerability to disulfide stress mediates disulfidoptosis. *Nature Cell Biology*. 2023; 25: 404–414.
- [7] Liu X, Olszewski K, Zhang Y, Lim EW, Shi J, Zhang X, *et al.* Cystine transporter regulation of pentose phosphate pathway dependency and disulfide stress exposes a targetable metabolic vulnerability in cancer. *Nature Cell Biology*. 2020; 22: 476–486.
- [8] Joly JH, Delfarah A, Phung PS, Parrish S, Graham NA. A synthetic lethal drug combination mimics glucose deprivation-induced cancer cell death in the presence of glucose. *The Journal of Biological Chemistry*. 2020; 295: 1350–1365.
- [9] Ergin M, Caliskanturk M, Senat A, Akturk O, Erel O. Disulfide stress in carbon monoxide poisoning. *Clinical Biochemistry*. 2016; 49: 1243–1247.
- [10] Kaya B, Turhan U, Sezer S, Bestel A, Okumuş ZG, Dağ İ, *et al.* Maternal serum TXNDC5 levels and thiol/disulfide homeostasis in preeclamptic pregnancies. *The Journal of Maternal-Fetal & Neonatal Medicine*. 2020; 33: 671–676.
- [11] Ergin M, Aydin C, Yurt EF, Cakir B, Erel O. The Variation of

- Disulfides in the Progression of Type 2 Diabetes Mellitus. *Experimental and Clinical Endocrinology & Diabetes*. 2020; 128: 77–81.
- [12] Piras IS, Krate J, Delvaux E, Nolz J, Mastroeni DF, Persico AM, *et al.* Transcriptome Changes in the Alzheimer's Disease Middle Temporal Gyrus: Importance of RNA Metabolism and Mitochondria-Associated Membrane Genes. *Journal of Alzheimer's Disease*. 2019; 70: 691–713.
- [13] Langfelder P, Horvath S. WGCNA: an R package for weighted correlation network analysis. *BMC Bioinformatics*. 2008; 9: 559.
- [14] Ru B, Wong CN, Tong Y, Zhong JY, Zhong SSW, Wu WC, *et al.* TISIDB: an integrated repository portal for tumor-immune system interactions. *Bioinformatics*. 2019; 35: 4200–4202.
- [15] Wishart DS, Feunang YD, Guo AC, Lo EJ, Marcu A, Grant JR, *et al.* DrugBank 5.0: a major update to the DrugBank database for 2018. *Nucleic Acids Research*. 2018; 46: D1074–D1082.
- [16] Yu H, Jiang X, Lin X, Zhang Z, Wu D, Zhou L, *et al.* Hippocampal Subcellular Organelle Proteomic Alteration of Copper-Treated Mice. *Toxicological Sciences*. 2018; 164: 250–263.
- [17] Poljšak B, Kovač V, Špalj S, Milisav I. The Central Role of the NAD⁺ Molecule in the Development of Aging and the Prevention of Chronic Age-Related Diseases: Strategies for NAD⁺ Modulation. *International Journal of Molecular Sciences*. 2023; 24: 2959.
- [18] Federico A, Cardaioli E, Da Pozzo P, Formichi P, Gallus GN, Radi E. Mitochondria, oxidative stress and neurodegeneration. *Journal of the Neurological Sciences*. 2012; 322: 254–262.
- [19] Singh A, Kukreti R, Saso L, Kukreti S. Oxidative Stress: A Key Modulator in Neurodegenerative Diseases. *Molecules*. 2019; 24: 1583.
- [20] Wu MF, Yin JH, Hwang CS, Tang CM, Yang DI. NAD attenuates oxidative DNA damages induced by amyloid beta-peptide in primary rat cortical neurons. *Free Radical Research*. 2014; 48: 794–805.
- [21] Li WX, Li GH, Tong X, Yang PP, Huang JF, Xu L, *et al.* Systematic metabolic analysis of potential target, therapeutic drug, diagnostic method and animal model applicability in three neurodegenerative diseases. *Aging*. 2020; 12: 9882–9914.
- [22] Zheng JJ, Li WX, Liu JQ, Guo YC, Wang Q, Li GH, *et al.* Low expression of aging-related NRXN3 is associated with Alzheimer disease: A systematic review and meta-analysis. *Medicine*. 2018; 97: e11343.
- [23] Khatib T, Chisholm DR, Whiting A, Platt B, McCaffery P. Decay in Retinoic Acid Signaling in Varied Models of Alzheimer's Disease and In-Vitro Test of Novel Retinoic Acid Receptor Ligands (RAR-Ms) to Regulate Protective Genes. *Journal of Alzheimer's Disease*. 2020; 73: 935–954.
- [24] Chen F, Bai J, Zhong S, Zhang R, Zhang X, Xu Y, *et al.* Molecular Signatures of Mitochondrial Complexes Involved in Alzheimer's Disease via Oxidative Phosphorylation and Retrograde Endocannabinoid Signaling Pathways. *Oxidative Medicine and Cellular Longevity*. 2022; 2022: 9565545.
- [25] Giannos P, Prokopidis K, Raleigh SM, Kelaiditi E, Hill M. Altered mitochondrial microenvironment at the spotlight of musculoskeletal aging and Alzheimer's disease. *Scientific Reports*. 2022; 12: 11290.
- [26] Navarro L, Gómez-Carballa A, Pischedda S, Montoto-Louzao J, Viz-Lasheras S, Camino-Mera A, *et al.* Sensogenomics of music and Alzheimer's disease: An interdisciplinary view from neuroscience, transcriptomics, and epigenomics. *Frontiers in Aging Neuroscience*. 2023; 15: 1063536.
- [27] Linnertz C, Lutz MW, Ervin JF, Allen J, Miller NR, Welsh-Bohmer KA, *et al.* The genetic contributions of SNCA and LRRK2 genes to Lewy Body pathology in Alzheimer's disease. *Human Molecular Genetics*. 2014; 23: 4814–4821.
- [28] Wang Q, Tian Q, Song X, Liu Y, Li W. SNCA Gene Polymorphism may Contribute to an Increased Risk of Alzheimer's Disease. *Journal of Clinical Laboratory Analysis*. 2016; 30: 1092–1099.
- [29] Bai Q, Wei X, Burton EA. Expression of a 12-kb promoter element derived from the zebrafish enolase-2 gene in the zebrafish visual system. *Neuroscience Letters*. 2009; 449: 252–257.
- [30] Liu L, Wu Q, Zhong W, Chen Y, Zhang W, Ren H, *et al.* Microarray Analysis of Differential Gene Expression in Alzheimer's Disease Identifies Potential Biomarkers with Diagnostic Value. *Medical Science Monitor*. 2020; 26: e919249.
- [31] Sekaran K, Alsamman AM, George Priya Doss C, Zayed H. Bioinformatics investigation on blood-based gene expressions of Alzheimer's disease revealed ORAI2 gene biomarker susceptibility: An explainable artificial intelligence-based approach. *Metabolic Brain Disease*. 2023; 38: 1297–1310.
- [32] Sarper N, Zengin E, Jakobs C, Salomons GS, Mc Wameling M, Ralser M, *et al.* Mild hemolytic anemia, progressive neuromotor retardation and fatal outcome: a disorder of glycolysis, triose-phosphate isomerase deficiency. *The Turkish Journal of Pediatrics*. 2013; 55: 198–202.
- [33] Peinado MÁ, Hernández R, Peragón J, Ovelleiro D, Pedrosa JÁ, Blanco S. Proteomic characterization of nitrated cell targets after hypobaric hypoxia and reoxygenation in rat brain. *Journal of Proteomics*. 2014; 109: 309–321.
- [34] Yang GJ, Tao F, Zhong HJ, Yang C, Chen J. Targeting PGAM1 in cancer: An emerging therapeutic opportunity. *European Journal of Medicinal Chemistry*. 2022; 244: 114798.
- [35] Kommaddi RP, Das D, Karunakaran S, Nanguneri S, Bapat D, Ray A, *et al.* A β mediates F-actin disassembly in dendritic spines leading to cognitive deficits in Alzheimer's disease. *The Journal of Neuroscience*. 2018; 38: 1085–1099.
- [36] Heredia L, Helguera P, de Olmos S, Kedikian G, Solá Vigo F, LaFerla F, *et al.* Phosphorylation of actin-depolymerizing factor/cofilin by LIM-kinase mediates amyloid beta-induced degeneration: a potential mechanism of neuronal dystrophy in Alzheimer's disease. *The Journal of Neuroscience*. 2006; 26: 6533–6542.
- [37] Fox J, Lu Z, Barrows L. Thiol-disulfide Oxidoreductases TRX1 and TMX3 Decrease Neuronal Atrophy in a Lentiviral Mouse Model of Huntington's Disease. *PLoS Currents*. 2015; 7: ecur-rents.hd.b966ec2eca8e2d89d2bb4d020be4351e.
- [38] Liu Q, Wang S, Hao Y, Li J, Li W, Zhang Y, *et al.* Active Compounds and Targets of Yuanzhi Powder in Treating Alzheimer's Disease and Its Relationship with Immune Infiltration Based on HPLC Fingerprint and Network Pharmacology. *Evidence-based Complementary and Alternative Medicine*. 2022; 2022: 3389180.
- [39] Kolaczowska E, Kubes P. Neutrophil recruitment and function in health and inflammation. *Nature Reviews. Immunology*. 2013; 13: 159–175.
- [40] Scali C, Proserpi C, Bracco L, Piccini C, Baronti R, Ginestroni A, *et al.* Neutrophils CD11b and fibroblasts PGE(2) are elevated in Alzheimer's disease. *Neurobiology of Aging*. 2002; 23: 523–530.
- [41] Cruz Hernández JC, Bracko O, Kersbergen CJ, Muse V, Haft-Javaherian M, Berg M, *et al.* Neutrophil adhesion in brain capillaries reduces cortical blood flow and impairs memory function in Alzheimer's disease mouse models. *Nature Neuroscience*. 2019; 22: 413–420.
- [42] Chitu V, Biundo F, Shlager GGL, Park ES, Wang P, Gulinello ME, *et al.* Microglial Homeostasis Requires Balanced CSF-1/CSF-2 Receptor Signaling. *Cell Reports*. 2020; 30: 3004–3019.e5.
- [43] Hu B, Duan S, Wang Z, Li X, Zhou Y, Zhang X, *et al.* Insights Into the Role of CSF1R in the Central Nervous System and Neu-

- rological Disorders. *Frontiers in Aging Neuroscience*. 2021; 13: 789834.
- [44] Henry RJ, Ritzel RM, Barrett JP, Doran SJ, Jiao Y, Leach JB, *et al.* Microglial Depletion with CSF1R Inhibitor During Chronic Phase of Experimental Traumatic Brain Injury Reduces Neurodegeneration and Neurological Deficits. *The Journal of Neuroscience*. 2020; 40: 2960–2974.
- [45] Perea JR, Lleó A, Alcolea D, Fortea J, Ávila J, Bolós M. Decreased CX3CL1 Levels in the Cerebrospinal Fluid of Patients With Alzheimer’s Disease. *Frontiers in Neuroscience*. 2018; 12: 609.
- [46] Rogers JT, Morganti JM, Bachstetter AD, Hudson CE, Peters MM, Grimmig BA, *et al.* CX3CR1 deficiency leads to impairment of hippocampal cognitive function and synaptic plasticity. *The Journal of Neuroscience*. 2011; 31: 16241–16250.
- [47] Leng F, Edison P. Neuroinflammation and microglial activation in Alzheimer disease: where do we go from here? *Nature Reviews. Neurology*. 2021; 17: 157–172.
- [48] Zhang XF, Zhao YF, Zhu SW, Huang WJ, Luo Y, Chen QY, *et al.* CXCL1 Triggers Caspase-3 Dependent Tau Cleavage in Long-Term Neuronal Cultures and in the Hippocampus of Aged Mice: Implications in Alzheimer’s Disease. *Journal of Alzheimer’s Disease*. 2015; 48: 89–104.
- [49] Ho T, Ahmadi S, Kerman K. Do glutathione and copper interact to modify Alzheimer’s disease pathogenesis? *Free Radical Biology & Medicine*. 2022; 181: 180–196.
- [50] Squitti R, Ghidoni R, Siotto M, Ventriglia M, Benussi L, Paterlini A, *et al.* Value of serum nonceruloplasmin copper for prediction of mild cognitive impairment conversion to Alzheimer disease. *Annals of Neurology*. 2014; 75: 574–580.
- [51] Esmieu C, Guettas D, Conte-Daban A, Sabater L, Faller P, Hureau C. Copper-Targeting Approaches in Alzheimer’s Disease: How To Improve the Fallouts Obtained from in Vitro Studies. *Inorganic Chemistry*. 2019; 58: 13509–13527.
- [52] Choi JM, Park HS, He MT, Kim YS, Kim HY, Lee AY, *et al.* Membrane-Free Stem Cells and Pyridoxal 5’-Phosphate Synergistically Enhance Cognitive Function in Alzheimer’s Disease Mouse Model. *Antioxidants*. 2022; 11: 601.
- [53] McCarty MF, O’Keefe JH, DiNicolantonio JJ. A diet rich in taurine, cysteine, folate, B₁₂ and betaine may lessen risk for Alzheimer’s disease by boosting brain synthesis of hydrogen sulfide. *Medical Hypotheses*. 2019; 132: 109356.
- [54] Corcoran JPT, So PL, Maden M. Disruption of the retinoid signalling pathway causes a deposition of amyloid beta in the adult rat brain. *The European Journal of Neuroscience*. 2004; 20: 896–902.
- [55] Bonhomme D, Pallet V, Dominguez G, Servant L, Henkous N, Lafenêtre P, *et al.* Retinoic acid modulates intrahippocampal levels of corticosterone in middle-aged mice: consequences on hippocampal plasticity and contextual memory. *Frontiers in Aging Neuroscience*. 2014; 6: 6.
- [56] Biyong EF, Tremblay C, Leclerc M, Caron V, Alfos S, Helbling JC, *et al.* Role of Retinoid X Receptors (RXRs) and dietary vitamin A in Alzheimer’s disease: Evidence from clinicopathological and preclinical studies. *Neurobiology of Disease*. 2021; 161: 105542.
- [57] Wang SSS, Good TA, Rymer DL. The influence of phospholipid membranes on bovine calcitonin peptide’s secondary structure and induced neurotoxic effects. *The International Journal of Biochemistry & Cell Biology*. 2005; 37: 1656–1669.
- [58] Kharechkina E, Nikiforova A, Kruglov A. NAD(H) Regulates the Permeability Transition Pore in Mitochondria through an External Site. *International Journal of Molecular Sciences*. 2021; 22: 8560.
- [59] Rainer M, Kraxberger E, Haushofer M, Mucke HA, Jellinger KA. No evidence for cognitive improvement from oral nicotinamide adenine dinucleotide (NADH) in dementia. *Journal of Neural Transmission*. 2000; 107: 1475–1481.
- [60] Ventriglia M, Brewer GJ, Simonelli I, Mariani S, Siotto M, Buccosi S, *et al.* Zinc in Alzheimer’s Disease: A Meta-Analysis of Serum, Plasma, and Cerebrospinal Fluid Studies. *Journal of Alzheimer’s Disease*. 2015; 46: 75–87.
- [61] Squitti R, Pal A, Picozza M, Avan A, Ventriglia M, Rongioletti MC, *et al.* Zinc Therapy in Early Alzheimer’s Disease: Safety and Potential Therapeutic Efficacy. *Biomolecules*. 2020; 10: 1164.